

A next-generation LHC heavy-ion experiment

List of authors in appendix

Abstract

The present document discusses plans for a compact, next-generation multi-purpose detector at the LHC as a follow-up to the present ALICE experiment. The aim is to build a nearly massless barrel detector consisting of truly cylindrical layers based on curved wafer-scale ultra-thin silicon sensors with MAPS technology, featuring an unprecedented low material budget of 0.05% X_0 per layer, with the innermost layers possibly positioned inside the beam pipe. In addition to superior tracking and vertexing capabilities over a wide momentum range down to a few tens of MeV/ c , the detector will provide particle identification via time-of-flight determination with about 20 ps resolution. In addition, electron and photon identification will be performed in a separate shower detector. The proposed detector is conceived for studies of pp, pA and AA collisions at luminosities a factor of 20 to 50 times higher than possible with the upgraded ALICE detector, enabling a rich physics program ranging from measurements with electromagnetic probes at ultra-low transverse momenta to precision physics in the charm and beauty sector.

Geneva, Switzerland

December 18, 2018

Contents

1	Introduction	3
2	Detector concept	4
2.1	Detector technology	4
2.2	Detector layout and main parameters	5
2.3	Tracking performance	7
3	Physics potential	8
3.1	Heavy flavour and quarkonia	8
3.2	Low-mass dileptons	10
3.2.1	The low mass continuum, $0 < m < 3$ GeV	10
3.2.2	Chiral symmetry restoration and the temperature of the hot QGP fireball	11
3.3	Soft and ultra-soft photons	11
3.4	Other topics	12

1 Introduction

With this document, we express our interest for a new LHC experiment, dedicated to the high-statistics study of the production of heavy flavour hadrons and of the soft electromagnetic and hadronic radiation produced in high-energy proton-proton and nuclear collisions. The apparatus would be centered on an ultra-low-mass silicon tracker, made with Complementary Metal-Oxide-Silicon (CMOS) Monolithic Active Pixel Sensors (MAPS) technology. Such an experiment could be installed during the LHC Long Shutdown 4 (LS4), at the Interaction Point 2 (IP2), where the ALICE experiment is currently installed.

The ALICE Collaboration is completing the construction of an upgraded Inner Tracking System (ITS2) with seven layers of CMOS MAPS, to be installed during LS2 [1]. Recent advances in this technology have made possible the fabrication of wafer-scale ultra-thin silicon detectors, and the ALICE Collaboration is currently considering a further upgrade (ITS3) in which the three innermost layers of ITS2 would be replaced with three truly cylindrical layers of such detectors, with a material budget of only 0.05% X_0 per layer [2].

This novel technology opens up the possibility of constructing a new, all-silicon tracker, with unprecedented low mass, that would allow reaching down to an ultra-soft region of phase space, to measure the production of very-low transverse momentum lepton pairs, photons and hadrons at the LHC. The detector would consist of a barrel and two end-caps made of layers of ultra-thin Si-sensors and cover the rapidity region $|\eta| < 4$. The ultra-low material thickness, combined with the placement of the first detector layers either inside the beam pipe or at a very close distance from its outer wall, would allow charged particle detection at transverse momenta of the order of a few tens of MeV/c.

The excellent timing resolution ($\simeq 20$ ps) achievable with CMOS detectors will provide particle identification information. Electrons at low momentum (< 500 MeV/c) will be separated from hadrons using time-of-flight information while, at higher momenta, electrons and photons will be identified in a dedicated shower detector. Removable converter structures will also allow the measurement of photons with the conversion method.

Such an experiment would, for instance, allow to measure the primordial electromagnetic radiation emitted by the Quark-Gluon Plasma (QGP) produced in nuclear collisions, providing key information for the understanding of the emergent properties of QCD matter. More generally, it would open a new window for the study of soft phenomena in hadronic collisions, allowing to address fundamental physics questions that could not be tackled so far.

The high-rate capabilities of MAPS will allow the experiment to run at significantly (a factor 20 to 50) higher luminosities than the upgraded ALICE experiment. It could therefore exploit all pA and AA luminosities that could be reached by accelerating ions from light to very heavy in the LHC [3].

The detector concept discussed in this document provides unprecedented physics performance for heavy flavour studies, enabling the measurement of the production of exotic quarkonia and Multiply Heavy Flavoured (MHF) baryons and mesons in pp, p-A and nuclear collisions, for which theoretical uncertainties span across orders of magnitude, providing a significant new window on the properties of the Quark-Gluon Plasma.

The current ideas for a possible layout are presented in section 2 and some of the areas where such an experiment would have a significant impact are discussed in section 3.

2 Detector concept

In the following we describe the key technologies, the conceptual layout and the main features of the proposed experimental apparatus, which is entirely based on CMOS technology.

2.1 Detector technology

CMOS technology, which fueled the rapid growth of the information technology industry in the past 50 years, has also played and continues to play a crucial role in the remarkable development of detectors for High-Energy Physics (HEP) experiments. The amazing evolution of CMOS transistors in terms of speed, integration and cost decrease, allowed a continuous increase of density, complexity and performance of the front-end and readout circuits for HEP detectors. With the advent of CMOS MAPS, where the sensing layer and its readout circuitry are combined in a single integrated circuit, CMOS became also the technology for a new generation of vertex and tracking detectors. An important example of such an approach is represented by the new ALICE Inner Tracking System (ITS2) [1], which is based on a MAPS device, named ALPIDE, covering about 10 m² of area with about 12.5 billion pixels.

The development of ALPIDE represents a quantum leap in the field of CMOS MAPS for single-particle detection, reaching unprecedented performance in terms of signal/noise ratio, spatial resolution, material budget and readout speed. Still, further significant improvements are possible by fully exploiting the rapid progress

that this technology is making in the fields of imaging and time-of-flight measurements for consumer applications.

One of the features offered recently by CMOS imaging sensor technologies, called stitching, will allow developing a new generation of large-size MAPS with an area of up to $14\text{ cm} \times 14\text{ cm}$, for 200 mm wafer processes, and up to $21\text{ cm} \times 21\text{ cm}$, for 300 mm wafer processes. Moreover, the reduction of the sensor thickness to values of about 20-40 μm will open the possibility of exploiting the flexible nature of silicon to implement large-area curved sensors. In this way, it will become possible to build cylindrical layers of silicon-only sensors, which will enable a dramatic reduction of the detector material thickness [2].

CMOS technology is also currently revolutionizing the field of 3D imaging, which has become a key sensing technology in a wide range of LiDAR (Light Detection And Ranging) applications in the field of robotic, automotive, medical and spacecraft systems. Time-of-flight (TOF) imagers based on CMOS Single Photon Avalanche Diodes (SPADs) feature very small pixel pitches, $O(40\text{ }\mu\text{m} \times 40\text{ }\mu\text{m})$, and very high time resolution. Such a technology can be further optimized and tailored towards the measurement of minimum ionizing particles with a time resolution of the order of a few tens of picoseconds.

2.2 Detector layout and main parameters

The view of the experimental apparatus is shown in Fig. 1. The detector, which covers the pseudorapidity region of $|\eta| < 4$ over the full azimuth, has a very compact layout with radial and longitudinal dimensions of 1.2 m and 4 m, respectively. It consists of a central barrel and two end-caps, which are embedded in a solenoid magnet (not shown in Fig. 1). The moderately weak solenoidal field (0.5 T) of the ALICE magnet seems adequate to meet the requirements of high tracking efficiency at very low transverse momentum (a few tens of MeV/c) while preserving very good relative momentum resolution ($\approx 2\%$) at high transverse momentum ($p_T \approx 30\text{ GeV}/c$). However, the option of a magnet with a larger magnetic field (1 T or larger) will also be considered.

The central barrel, which covers the pseudorapidity region $|\eta| < 1.4$, consists of (from the inside out) an Inner Tracker (IT), with 3 layers located inside the beam pipe, the Outer Tracker (OT) with 7 layers, a Time-Of-Flight (TOF) detector for the identification of hadrons, as well as electrons at very low transverse momentum ($p_T < 500\text{ MeV}/c$), and an electromagnetic Shower Pixel Detector (SPD) for the identification of electrons and photons ($p_T > 500\text{ MeV}/c$). The two endcaps, which extend the acceptance to the pseudorapidity region $1.4 < |\eta| < 4$, contain each 4 disks in the IT, 6 disks in the OT and one disk in the SPD.

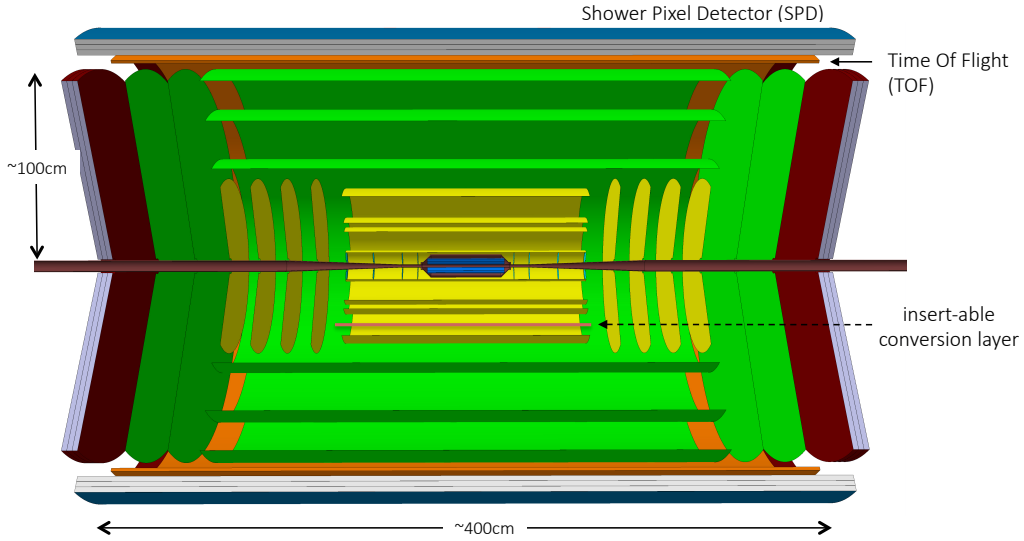


Figure 1: Longitudinal view of the experimental apparatus. The detector is embedded in a solenoid magnet (not shown in the figure). The central barrel, which covers the pseudorapidity region $|\eta| < 1.4$, is composed of the IT, inside the beampipe (blue layers in the figure), the OT (yellow and green layers), the TOF (orange layers) and the SPD (outermost blue layers). Two endcaps, each consisting of a set of tracking disks and an SPD disk, extend the rapidity coverage to the region $|\eta| < 4$.

The IT barrel is based on curved wafer-scale ultra-thin CMOS MAPS arranged in truly cylindrical layers, featuring an unprecedented low material budget of $0.05\% X_0$ per layer, with the innermost layer positioned at only 18 mm radial distance from the beam line. The pixel sensor contains approximately 10^6 pixels per square centimeter, each measuring about $10\ \mu\text{m} \times 10\ \mu\text{m}$, featuring a position resolution of better than $3\ \mu\text{m}$. The IT layers will be located either in the secondary vacuum of a larger vacuum chamber, as shown in Fig. 1, or outside the beam pipe, with the innermost layers at a radial distance of 2 mm from its outer wall. Four end-cap disks on each side complement the central barrel layers. A system of seven barrel layers and six endcap disks form the OT. They are based on the same technology as the sensors for the vertex detector, but their pixel size is increased to about $30\ \mu\text{m} \times 30\ \mu\text{m}$ in order to reduce the power density. These layers will provide a spatial resolution of about $5\ \mu\text{m}$. The material budget of the OT layers will be about $0.5\% X_0$ per layer.

A TOF detector consisting of three layers of CMOS MAPS with time resolution of the order of 20 ps will surround the central tracker. Low-Gain Avalanche Detectors (LGAD) featuring such a time precision, which are being developed for

the phase-II upgrade of the ATLAS and CMS experiments, represent a viable option. Given the moderately low radiation levels at the location of the time-of-flight system (10^{12} 1 MeV $n_{\text{eq}}/\text{cm}^2$), CMOS SPADs also represent a very promising technology. These detectors are based on arrays of avalanche photodiodes reverse-biased above their breakdown voltage. SPAD detectors of recent generation feature a time jitter of tens of picoseconds. The number of layers needed for the realization of the TOF detector will depend on the time resolution and spatial fill factor achieved in the single layer.

The SPD is based on a stack-up of a few layers made of a dense passive material, e.g. lead, interleaved with layers of high-granularity pixel sensors, which allow counting individual particles generated in a shower. Electrons and positrons will be distinguished from photons by the presence of a track in the tracking layers. The contamination from pions will be very small due to the large ratio between the nuclear interaction length and the radiation length of lead ($\lambda_n/X_0 \simeq 30$).

2.3 Tracking performance

The tracking performance of this detector has been studied using a fast Monte Carlo tool. The code, which accounts for multiple scattering, detector occupancy and deterministic energy loss, provides accurate determination of the tracking resolution as a function of the detector configuration for both the spatial and the momentum components and a reliable estimate of the tracking efficiency.

An important measure of the achieved tracking precision is the track impact-parameter resolution, defined as the dispersion of the distribution of the Distance of Closest Approach (DCA) of the reconstructed tracks to their production vertex. It is the parameter that defines the capability of a vertex detector to separate secondary vertices of heavy-flavour decays from the interaction vertex. Two alternative configurations have been studied. In the first configuration, the three IT layers are contained inside the beam vacuum chamber, while the innermost OT layer is located outside of it at a radial distance of about 2 mm from the outer wall. In the second configuration the IT layers are located outside the beam pipe with the innermost layers at about 2 mm from the outer wall. The radial arrangement of the IT layers is identical for the two configurations. A comparison of the impact-parameter resolution for the two configurations is shown in Fig. 2 for at typical pseudorapidity $|\eta| = 0.5$. Owing to its nearly zero mass, the detector exhibits a spectacular vertexing performance, with an impact parameter resolution that is below $10 \mu\text{m}$ for $p_T \simeq 1 \text{ GeV}/c$ and remains below $100 \mu\text{m}$ down to $p_T \simeq 0.1 \text{ GeV}/c$.

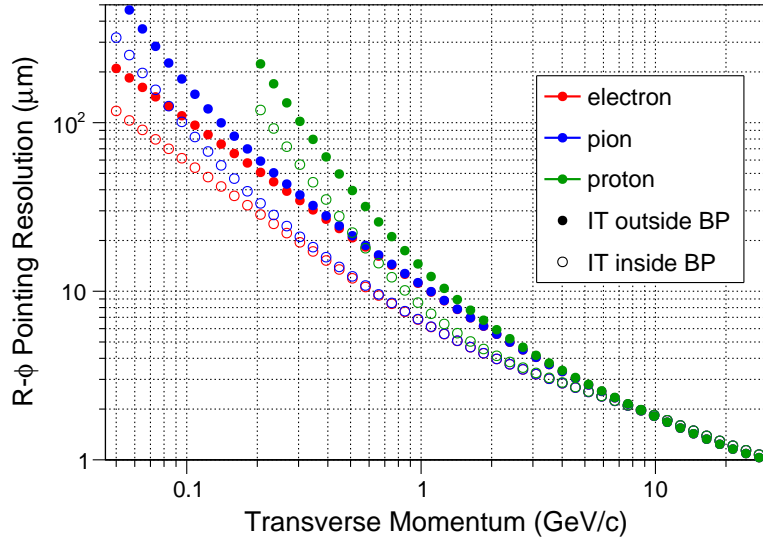


Figure 2: Impact parameter resolution for primary electrons, charged pions and protons as a function of the transverse momentum for two configurations of the IT: inside the beam pipe (empty circles) and outside the beam pipe (filled circles).

3 Physics potential

The ability to measure the production of leptons, photons and identified hadrons down to p_T scales of the order of a few tens of MeV/c , would provide significant advances in several areas. In the following, we list only some of the physics topics that would dramatically benefit from such an apparatus.

3.1 Heavy flavour and quarkonia

The unique tracking and vertexing capabilities of the proposed apparatus, combined with its high-luminosity capabilities, will provide an ideal tool for a comprehensive campaign of high-precision measurements of the production of open and hidden heavy flavour particles in nuclear collisions. Below, we list some examples of measurements where the proposed experiment will have a crucial impact.

The suppression of the production of quarkonia due to Debye screening of the strong interaction was one of the first predicted signatures of colour deconfinement [4]. Anomalous suppression of the production of J/ψ mesons (beyond the level that could be explained by conventional models, such as the interaction of the

J/ψ with comoving hadrons) was experimentally observed in nuclear collisions at the CERN Super Proton Synchrotron [5]. Measurements on Au-Au collisions at RHIC revealed similar levels of suppression as at the SPS [6].

Data from Pb-Pb collisions at the LHC have revealed a new regime for J/ψ production [7]: at the LHC the suppression is reduced compared to lower energies and, unlike at lower energies, it is very weakly dependent on the centrality of the collision and instead of decreasing, it increases with increasing p_T . Such observations are consistent with the presence of a significant contribution at the LHC from a novel mechanism, which had been proposed in [8], for a recent review see [9], for quarkonium production via statistical hadronization of initially uncorrelated heavy quark pairs at the phase boundary. Alternatively, a mechanism of continuous creation and destruction of charmonia in the QGP was proposed in [10]. In this new regime for J/ψ production the above mentioned p_T dependence arises naturally, as predicted in [11]. If the above picture is correct, measurements of exotic hadrons would provide a direct window on hadron formation from a deconfined Quark-Gluon Plasma, and spectacular effects would be expected for Multiply Heavy Flavoured (MHF) baryons and mesons. In such a scenario, the yields of MHF baryons relative to the number of produced charm quarks are predicted to be enhanced in AA relative to pp collisions. First predictions in this area were made in [12], recent calculations are discussed in [13, 14, 15, 16]. Enhancements are expected by as much as a factor 10^2 for the recently discovered Ξ_{cc} baryon and even by as much as a factor 10^3 for the as yet undiscovered Ω_{ccc} baryon. The observation and precise quantification of such effects would represent a quantum jump for the study of the properties of deconfined matter. The observation of the effect in MHF hadrons would provide a key confirmation of the current interpretation of the LHC quarkonium results and open a crucial new window to study the mechanisms of hadron formation from a deconfined Quark-Gluon Plasma. Such studies are currently way beyond reach. The detection of MHF baryons at the LHC requires nucleon-nucleon luminosities of the order of 1 fb^{-1} [17], with excellent tracking and secondary vertex and particle identification capabilities down to low transverse momenta to enable the reconstruction of complex cascades of weak decays of heavy flavour hadrons. The apparatus discussed in this document would provide the ideal detector for such measurements, combining ultra-low-mass tracking over a wide momentum range, particle identification and high-speed capabilities. Nucleon-nucleon luminosities in the fb^{-1} range could be accumulated at the LHC in a few weeks with the use of lighter nuclei such as Xe or Kr [3], bringing such measurements well within reach.

The proposed detector would also significantly enhance the capability for quarkonium physics. The systematics of charmonium production cannot be fully understood without a precise separation of prompt charmonia from those originating

from B decays as well as a quantitative determination of the production yields of low transverse momentum χ_c states, that can decay strongly into prompt J/ψ , but are expected to be much more fragile, due to the significantly smaller binding energy. The separation of prompt charmonia from secondary charmonia from B decays in the proposed apparatus will be excellent, and the high luminosity should make even the rare $\psi(2S)$ abundant. The detection of χ_c states involves the identification of a low-energy (300-400 MeV) photon in addition to a J/ψ meson. Low-energy photons can be measured with high efficiency in the SPD. A resolution of about 5% around 400 MeV is required, corresponding to $\frac{\delta E_\gamma}{E_\gamma} \approx 3\% / \sqrt{E_\gamma(\text{GeV})}$, which may be achievable in the SPD.

The proposed detector can also be used to shed new light on the nature and structure of the X, Y, Z charmonium-like states recently discovered, see, e.g., [18] and references therein. As a case in point we note that the X(3872) state which is well studied in pp collisions could be measured with precision also in nuclear collisions. Since this is a charmonium state, its yield is expected to be particularly enhanced at low transverse momenta ($p_T < 4 \text{ GeV}/c$) [19]. It would also be very interesting to perform a precision comparison of the transverse momentum spectra of particles of similar mass, but very different binding energies, such as $\psi(2S)$ and X(3872).

3.2 Low-mass dileptons

3.2.1 THE LOW MASS CONTINUUM, $0 < m < 3 \text{ GeV}$

The strongly-interacting medium is expected to emit electromagnetic radiation during a significant part of its lifetime. At colliders, signals of an excess of dileptons with respect to the expectations from known hadronic sources have been observed both at RHIC [20, 21, 22] and with still low significance at the LHC [23]. For LHC Run3 and Run4 the ALICE collaboration will upgrade its detector [24] resulting in significant improvements for low-mass dilepton measurements compared to the results from the present RHIC and LHC experiments.

The nearly massless detector with high-precision tracking and vertexing and very high rate capability, discussed in this document, would allow pushing down in transverse momentum very close to the natural scale determined by the inverse radius of the system (about 100 MeV/c in pp collisions, about 10 MeV/c in Pb-Pb collisions), which would represent the "ultimate" dilepton experiment.

The very low mass and p_T cutoff would allow testing theoretical predictions in the region of phase space, currently beyond reach, where most of the radiation is emitted.

3.2.2 CHIRAL SYMMETRY RESTORATION AND THE TEMPERATURE OF THE HOT QGP FIREBALL

Up to now, no direct experimental evidence exists for the restoration of chiral symmetry in the hot and dense phase formed during a relativistic nucleus-nucleus collision. Indeed, the enhanced low-mass dilepton continuum found at the SPS, RHIC, and LHC, can be described well by assuming that the ρ meson broadens in the medium without mass change [25, 26, 27, 22, 23]. With an essentially massless detector as described above one can take an entirely new approach, based on a precision measurement of the thermal dilepton continuum starting from the ρ meson and reaching up to masses of about 1.6 GeV. Guidance comes from inspecting the light flavor section of Fig. 51.3 of the latest PDG Review of Particle Physics [28]. Here one can see that the R factor obtained from e^+e^- collisions and representing the ‘vacuum’ in this context has a clear minimum near masses of 1.26 GeV, the mass of the a_1 meson. This meson is generally considered the chiral partner of the ρ meson and as such does not couple to e^+e^- pairs, hence the minimum. The idea for the proposed measurement is then to study this mass region in pp, p-Pb and Pb-Pb collisions to see whether the minimum near 1.26 GeV fills in as one goes from minimum bias pp to central Pb-Pb collisions.

With the dramatic improvements in vertexing from the detector described above, it will be possible to quantitatively measure and tag/reject non-prompt dileptons, revealing the true thermal continuum. We note that the only other known background for this measurement is from Drell-Yan production which at LHC energies is estimated to be negligible. With this approach one could not only provide a crucial test for chiral symmetry restoration in the ρ - a_1 sector but also make a precision determination of the temperature of the QGP from the analysis of the mass spectrum in the 1.8 – 3 GeV region.

3.3 Soft and ultra-soft photons

Measurements of real soft photons are notoriously difficult due to the huge background from π^0 decays and electron bremsstrahlung. Available measurements in ultra-relativistic nuclear collisions typically extend down to around 1 GeV, see [29] and references therein. In the proposed ultra-low mass tracker soft real photons could be measured using the conversion method pioneered by ALICE [29]. This should extend the photon transverse momentum range into the region of 50 - 100 MeV/c, thereby allowing tests of current predictions for radiation from the QGP in completely uncharted regions of phase space.

Very low p_T photons ($1 \text{ MeV}/c < p_T^\gamma < 100 \text{ MeV}/c$) could be measured with a

special, small spectrometer at forward rapidity in the range $3.5 < |\eta| < 5$.

The measurement of very soft electromagnetic radiation in the p_T region below 100 MeV/c and approaching 1 MeV/c is of fundamental interest. The production of photons at such low transverse momenta arises as a consequence of the structure of all gauge theories, see, in particular, [30, 31, 32, 33, 34]. According to resulting soft theorems the number of soft (real) photons actually diverges towards low p_T , but, as discussed in [34], *"in a highly controlled manner that is central to the consistency of the underlying quantum field theory"*. It would be of prime importance to reach the experimental sensitivity to test this prediction. This would require measurements at very low p_T , below 10 MeV/c, which could be achieved with a high-rapidity photon spectrometer. It is intuitively clear that the $1/p_T$ divergence characteristic of photon bremsstrahlung and predicted by [30, 31] will eventually be reached, but at what level and at which value of p_T will depend on the size and structure of the system, possibly on its quark content [35].

To make progress in this area one would measure photon production for pp and pA and ultimately Pb-Pb collisions. To date there exist two such measurements for hadron-hadron collisions, [36] where photons from $p + \text{Be} \rightarrow \gamma + X$ at 450 GeV beam momentum were detected and from $K^+ + p \rightarrow \gamma + X$ [37] at 70 GeV/c beam momentum where photons down to a few MeV/c were detected. These results were analyzed by [38], in the framework of quark synchrotron radiation. It would be very important to follow up on this with a state-of-the-art measurement at the LHC.

3.4 Other topics

An ultra-low mass, high-resolution and high-rate experiment as discussed in this document, would also allow to make major contributions to other areas, not covered here, such as precision studies of spectral distortions at low transverse momenta, coherent pion production, hadronisation at very-low transverse momenta, disoriented chiral condensates, femtoscopy, fluctuations and diffusion of conserved charges as well as the search for dark photons.

References

- [1] B. Abelev *et al.*, “Upgrade of the ALICE Inner Tracking System Technical Design Report,” *CERN-LHCC-2013-024*.
- [2] A. Collaboration, “Expression of Interest for an ALICE ITS Upgrade in LS3,” *ALICE-PUBLIC-2018-013*, 2018.
- [3] Z. Citron, A. Dainese, J. F. Grosse-Oetringhaus, J. Jowett, Y.-J. Lee, U. Wiedemann, and M. A. Winn, “Future physics opportunities for high-density QCD at the LHC with heavy-ion and proton beams,” Tech. Rep. CERN-LPCC-2018-07, CERN, Geneva, 2018.
- [4] T. Matsui and H. Satz, “ J/ψ Suppression by Quark-Gluon Plasma Formation,” *Phys. Lett.*, vol. B178, pp. 416–422, 1986.
- [5] B. Alessandro *et al.*, “A New measurement of J/ψ suppression in Pb-Pb collisions at 158-GeV per nucleon,” *Eur. Phys. J.*, vol. C39, pp. 335–345, 2005.
- [6] A. Adare *et al.*, “ J/ψ Production vs Centrality, Transverse Momentum, and Rapidity in Au+Au Collisions at $\sqrt{s_{NN}} = 200$ GeV,” *Phys. Rev. Lett.*, vol. 98, p. 232301, 2007.
- [7] B. B. Abelev *et al.*, “Centrality, rapidity and transverse momentum dependence of J/ψ suppression in Pb-Pb collisions at $\sqrt{s_{NN}} = 2.76$ TeV,” *Phys. Lett.*, vol. B734, pp. 314–327, 2014.
- [8] P. Braun-Munzinger and J. Stachel, “(Non)thermal aspects of charmonium production and a new look at J/ψ suppression,” *Phys. Lett.*, vol. B490, pp. 196–202, 2000.
- [9] A. Andronic, P. Braun-Munzinger, K. Redlich, and J. Stachel, “Decoding the phase structure of QCD via particle production at high energy,” *Nature*, vol. 561, no. 7723, pp. 321–330, 2018.
- [10] R. L. Thews, M. Schroedter, and J. Rafelski, “Enhanced J/ψ production in deconfined quark matter,” *Phys. Rev.*, vol. C63, p. 054905, 2001.
- [11] X. Zhao and R. Rapp, “Medium Modifications and Production of Charmonia at LHC,” *Nucl. Phys.*, vol. A859, pp. 114–125, 2011.
- [12] F. Becattini, “Production of multiply heavy flavored baryons from quark gluon plasma in relativistic heavy ion collisions,” *Phys. Rev. Lett.*, vol. 95, p. 022301, 2005.
- [13] S. Cho *et al.*, “Exotic Hadrons from Heavy Ion Collisions,” *Prog. Part. Nucl. Phys.*, vol. 95, pp. 279–322, 2017.

- [14] J. Zhao, H. He, and P. Zhuang, “Searching for Ξ_{cc}^+ in Relativistic Heavy Ion Collisions,” *Phys. Lett.*, vol. B771, pp. 349–353, 2017.
- [15] H. He, Y. Liu, and P. Zhuang, “ Ω_{ccc} production in high energy nuclear collisions,” *Phys. Lett.*, vol. B746, pp. 59–63, 2015.
- [16] A. Andronic, P. Braun-Munzinger, B. Dönigus, M. Köhler, K. Redlich, and J. Stachel, *manuscript in preparation*.
- [17] R. Aaij *et al.*, “Observation of the doubly charmed baryon Ξ_{cc}^{++} ,” *Phys. Rev. Lett.*, vol. 119, p. 112001, Sep 2017.
- [18] A. Esposito, A. L. Guerrieri, F. Piccinini, A. Pilloni, and A. D. Polosa, “Four-Quark Hadrons: an Updated Review,” *Int. J. Mod. Phys.*, vol. A30, p. 1530002, 2015.
- [19] A. Andronic, P. Braun-Munzinger, M. Köhler, K. Redlich, and J. Stachel, *manuscript in preparation*.
- [20] J. Adam *et al.*, “Low- p_T e^+e^- pair production in Au+Au collisions at $\sqrt{s_{NN}} = 200$ GeV and U+U collisions at $\sqrt{s_{NN}} = 193$ GeV at STAR,” *Phys. Rev. Lett.*, vol. 121, no. 13, p. 132301, 2018.
- [21] J. Adam *et al.*, “Measurements of Dielectron Production in Au+Au Collisions at $\sqrt{s_{NN}} = 27, 39,$ and 62.4 GeV from the STAR Experiment,” 2018.
- [22] A. Adare *et al.*, “Dielectron production in Au+Au collisions at $\sqrt{s_{NN}} = 200$ GeV,” *Phys. Rev.*, vol. C93, no. 1, p. 014904, 2016.
- [23] S. Acharya *et al.*, “Measurement of dielectron production in central Pb-Pb collisions at $\sqrt{s_{NN}} = 2.76$ TeV,” 2018.
- [24] B. Abelev *et al.*, “Upgrade of the ALICE Experiment: Letter Of Intent,” *J. Phys.*, vol. G41, p. 087001, 2014.
- [25] R. Arnaldi *et al.*, “NA60 results on thermal dimuons,” *Eur. Phys. J.*, vol. C61, pp. 711–720, 2009.
- [26] D. Adamova *et al.*, “Modification of the rho-meson detected by low-mass electron-positron pairs in central Pb-Au collisions at 158-A-GeV/c,” *Phys. Lett.*, vol. B666, pp. 425–429, 2008.
- [27] R. Rapp, J. Wambach, and H. van Hees, “The Chiral Restoration Transition of QCD and Low Mass Dileptons,” *Landolt-Bornstein*, vol. 23, p. 134, 2010.
- [28] M. Tanabashi *et al.*, “Review of Particle Physics,” *Phys. Rev.*, vol. D98, no. 3, p. 030001, 2018.
- [29] J. Adam *et al.*, “Direct photon production in Pb-Pb collisions at $\sqrt{s_{NN}} = 2.76$ TeV,” *Phys. Lett.*, vol. B754, pp. 235–248, 2016.

- [30] F. Bloch and A. Nordsieck, “Note on the Radiation Field of the electron,” *Phys. Rev.*, vol. 52, pp. 54–59, 1937.
- [31] F. E. Low, “Bremsstrahlung of very low-energy quanta in elementary particle collisions,” *Phys. Rev.*, vol. 110, pp. 974–977, 1958.
- [32] R. N. Cahn, “Inclusive Photon Spectra and High-Energy Multiplicities,” *Phys. Rev. Lett.*, vol. 29, p. 1481, 1972.
- [33] V. Lysov, S. Pasterski, and A. Strominger, “Low’s Subleading Soft Theorem as a Symmetry of QED,” *Phys. Rev. Lett.*, vol. 113, no. 11, p. 111601, 2014.
- [34] A. Strominger, “Lectures on the Infrared Structure of Gravity and Gauge Theory,” 2017.
- [35] O. Nachtmann and A. Reiter, “The Vacuum Structure in QCD and Hadron - Hadron Scattering,” *Z. Phys.*, vol. C24, p. 283, 1984.
- [36] J. Antos *et al.*, “Soft photon production in 400-GeV/c p - Be collisions,” *Z. Phys.*, vol. C59, pp. 547–554, 1993.
- [37] P. V. Chliapnikov, E. A. De Wolf, A. B. Fenyuk, L. N. Gerdyukov, Y. Goldschmidt-Clermont, V. M. Ronzhin, and A. Weigend, “Observation of Direct Soft Photon Production in K^+p Interactions at 70-GeV/c,” *Phys. Lett.*, vol. 141B, pp. 276–280, 1984.
- [38] G. W. Botz, P. Haberl, and O. Nachtmann, “Soft photons in hadron hadron collisions: Synchrotron radiation from the QCD vacuum?,” *Z. Phys.*, vol. C67, pp. 143–158, 1995.

Author List

D. Adamová⁷², G. Aglieri Rinella²³, M. Agnello²¹, Z. Ahammed¹⁰², D. Aleksandrov⁶⁷, A. Alici^{5,39}, A. Alkin², T. Alt⁴⁷, I. Altsybeev⁸², D. Andreou²³, A. Andronic^{79,104}, F. Antinori⁴¹, P. Antonioli³⁹, H. Appelshäuser⁴⁷, R. Arnaldi⁴³, I.C. Arsene¹², M. Arslanok⁷⁸, R. Averbeck⁷⁹, M.D. Azmi¹⁰, X. Bai⁷⁹, R. Bailhache⁴⁷, R. Bala⁷⁵, L. Barioglio¹⁶, G.G. Barnaföldi¹⁰⁵, L.S. Barnby⁷¹, P. Bartalini⁴, K. Barth²³, S. Basu¹⁰³, F. Becattini¹⁸, C. Bedda⁵¹, I. Belikov⁹², F. Bellini²³, R. Bellwied⁹⁵, S. Beole¹⁶, L. Bergmann⁷⁸, R.A. Bertens⁹⁹, M. Besoiu⁵⁴, L. Betev²³, A. Bhatti⁷⁹, A. Bianchi¹⁶, L. Bianchi^{16,95}, J. Bielčik²⁵, J. Bielčíková⁷², A. Bilandzic^{77,87}, S. Biswas³, R. Biswas³, D. Blau⁶⁷, F. Bock²³, M. Bombara²⁶, M. Borri⁷¹, P. Braun-Munzinger⁷⁹, M. Bregant⁸⁹, G.E. Bruno²², M.D. Buckland⁹⁷, H. Buesching⁴⁷, S. Bufalino²¹, P. Buncic²³, J.B. Butt⁷, A. Caliva⁷⁹, P. Camerini¹⁵, F. Carnesecchi⁵, J. Castillo Castellanos⁹³, F. Catalano²⁰, S. Chapeland²³, M. Chartier⁹⁷, C. Cheshkov⁹¹, B. Cheynis⁹¹, V. Chibante Barroso²³, D.D. Chinellato⁹⁰, P. Chochula²³, T. Chujo¹⁰¹, C. Cicalo⁴⁰, F. Colamaria³⁸, D. Colella³⁸, M. Concas^{43,1}, Z. Conesa del Valle⁴⁶, G. Contin⁹⁷, J.G. Contreras²⁵, F. Costa²³, B. Dönigus⁴⁷, T. Dahms^{77,87}, A. Dainese⁴¹, J. Dainton⁹⁷, A. Danu⁵⁴, S. Das³, D. Das⁸⁰, S. Dash³⁴, A. Dash⁶⁵, G. David⁸³, A. De Caro¹³, G. de Cataldo³⁸, A. De Falco¹⁴, N. De Marco⁴³, S. De Pasquale¹³, S. Deb³⁵, D. Di Bari²², A. Di Mauro²³, T. Dietel⁹⁴, R. Divià²³, U. Dmitrieva⁵⁰, A. Dobrin²³, A.K. Dubey¹⁰², A. Dubla⁷⁹, D. Elia³⁸, B. Erazmus⁸⁵, A. Erokhin⁸², G. Eulisse²³, D. Evans⁸¹, L. Fabbietti^{77,87}, M. Faggin¹⁹, P. Fecchio²¹, A. Feliciello⁴³, G. Feofilov⁸², A. Fernández Téllez³⁰, A. Festanti²³, S. Floerchinger⁴⁹, P. Foka⁷⁹, S. Fokin⁶⁷, A. Franco³⁸, C. Furget⁶⁰, A. Furs⁵⁰, J. Gaardhøje⁶⁸, M. Gagliardi¹⁶, P. Ganoti⁶³, C. Garabatos⁷⁹, E. Garcia-Solis⁶, C. Gargiulo²³, P. Gasik⁷⁷, M.B. Gay Ducati⁵⁶, M. Germain⁸⁵, P. Ghosh¹⁰², P. Giubellino⁴³, P. Giubilato¹⁹, P. Glässel⁷⁸, V. Gonzalez⁷⁹, O. Grachov¹⁰³, A. Grigoryan¹, S. Grigoryan⁵⁸, F. Grosa²¹, J.F. Grosse-Oetringhaus²³, R. Guernane⁶⁰, T. Gunji¹⁰⁰, R. Gupta⁷⁵, A. Gupta⁷⁵, M.K. Habib⁷⁹, H. Hamagaki⁶², J.W. Harris¹⁰⁶, D. Hatzifotiadou^{5,39}, S.T. Heckel⁴⁷, E. Hellbär⁴⁷, H. Helstrup²⁴, T. Herman²⁵, H. Hillemanns²³, C. Hills⁹⁷, B. Hippolyte⁹², S. Hornung⁷⁹, P. Hristov²³, J.P. Iddon⁹⁷, S. Igotkin⁸², G. Innocenti²³, M. Ippolitov⁶⁷, M. Ivanov⁷⁹, A. Jacholkowski¹⁷, M. Jung⁴⁷, A. Jusko⁸¹, M.K. Köhler⁷⁸, S. Kabana⁸⁵, A. Kalweit²³, A. Karasu Uysal⁵⁹, T. Karavicheva⁵⁰, U. Kebschull⁵⁷, R. Keidel³², M. Keil²³, B. Ketzer²⁹, S.A. Khan¹⁰², A. Khanzadeev⁷³, Y. Kharlov⁶⁹, A. Khuntia³⁵, B. Kim⁴⁵, J. Kim⁷⁸, M. Kim^{45,78}, J. Klein⁴³, C. Klein⁴⁷, C. Klein-Bösing¹⁰⁴, S. Klewin⁷⁸, A. Kluge²³, M.L. Knichel²³, C. Kobdaj⁸⁶, M. Kofarago¹⁰⁵, P.J. Konopka²³, V. Kovalenko⁸², I. Králik⁵², M. Krüger⁴⁷, L. Kreis⁷⁹, M. Krivda⁸¹, F. Krizek⁷², M. Kroesen⁷⁸, E. Kryshen⁷³, V. Kučera^{45,72}, C. Kuhn⁹², L. Kumar⁷⁴, S. Kundu⁶⁵, S. Kuschpil⁷², M.J. Kweon⁴⁵, M. Kwon¹¹, Y. Kwon¹⁰⁷, P. Lévai¹⁰⁵, S.L. La Pointe²⁷, E. Laudi²³, T. Lazareva⁸², R. Lea¹⁵, L. Leardini⁷⁸, S. Lee¹¹, R.C. Lemmon⁷¹, R. Lietava⁸¹, B. Lim¹¹, V. Lindenstruth²⁷, A. Lindner³³, C. Lippmann⁷⁹, J. Liu⁹⁷, J. Lopez

Lopez⁷⁸, C. Lourenco²³, G. Luparello⁴⁴, S.M. Mahmood¹², A. Maire⁹², V. Manzari³⁸, Y. Mao⁴, A. Marín⁷⁹, M. Marchisone⁹¹, G.V. Margagliotti¹⁵, M. Marquard⁴⁷, P. Martinengo²³, S. Masciocchi⁷⁹, M. Maserà¹⁶, E. Masson⁸⁵, A. Mastroserio³⁸, A.M. Mathis^{77,87}, A. Matyja^{88,99}, M. Mazzilli²², M.A. Mazzoni⁴², L. Micheletti¹⁶, A.N. Mishra⁵⁵, D. Miskowicz⁷⁹, B. Mohanty⁶⁵, M. Mohisin Khan^{10,II}, A. Morsch²³, T. Mrnjavac²³, V. Muccifora³⁷, D. Mühlheim¹⁰⁴, S. Muhuri¹⁰², J.D. Mulligan^{61,106}, M.G. Munhoz⁸⁹, R.H. Munzer⁴⁷, H. Murakami¹⁰⁰, L. Musa²³, B. Naik³⁴, B.K. Nandi³⁴, R. Nania^{5,39}, T.K. Nayak^{65,102}, D. Nesterov⁸², G. Nicosia⁹⁸, S. Nikolaev⁶⁷, V. Nikulin⁷³, F. Noferini^{5,39}, J. Norman⁶⁰, A. Nyanin⁶⁷, V. Okorokov⁷⁰, C. Oppedisano⁴³, J. Otwinowski⁸⁸, K. Oyama⁶², M. Płoskoń⁶¹, Y. Pachmayer⁷⁸, A.K. Pandey³⁴, C. Pastore³⁸, J. Pawłowski⁷⁸, H. Pei⁴, T. Peitzmann⁵¹, D. Peresunko⁶⁷, M. Petrovici³³, R.P. Pezzi⁵⁶, S. Piano⁴⁴, E. Prakasa³⁶, S.K. Prasad³, R. Preghenella³⁹, F. Prino⁴³, C.A. Pruneau¹⁰³, I. Pshenichnov⁵⁰, M. Puccio¹⁶, J. Pucek²⁵, E. Quercigh²³, D. Röhrich⁹, L. Ramello²⁰, F. Rami⁹², S. Raniwala⁷⁶, R. Raniwala⁷⁶, R. Rath³⁵, I. Ravasenga²¹, A. Redelbach²⁷, K. Redlich^{64,III}, F. Reidt²³, K. Reygers⁷⁸, V. Riabov⁷³, P. Riedler²³, W. Riegler²³, D. Rischke⁴⁸, C. Ristea⁵⁴, S.P. Rode³⁵, M. Rodríguez Cahuantzi³⁰, D. Rohr²³, A. Rossi^{19,41}, R. Rui¹⁵, A. Rustamov⁶⁶, A. Rybicki⁸⁸, K. Šafařík^{23,25}, R. Sadikin³⁶, S. Sadovsky⁶⁹, R. Sahoo³⁵, P. Sahoo³⁵, P.K. Sahu⁵³, J. Saini¹⁰², V. Samsonov⁷³, P. Sarma²⁸, H.S. Scheid⁴⁷, R. Schicker⁷⁸, A. Schmäh⁷⁸, M.O. Schmidt⁷⁸, C. Schmidt⁷⁹, Y. Schutz^{23,92}, K. Schweda⁷⁹, E. Scomparin⁴³, J.E. Seger⁸, S. Senyukov⁹², A. Seryakov⁸², R. Shahoyan²³, N. Sharma⁷⁴, S. Siddhanta⁴⁰, T. Siemiarczuk⁶⁴, R. Singh⁶⁵, M. Sitta²⁰, H. Soltveit⁷⁸, M. Spyropoulou-Stassinaki⁶³, J. Stachel⁷⁸, T. Sugitate³¹, S. Sumowidagdo³⁶, X. Sun⁴, J. Takahashi⁹⁰, C. Terrevoli^{19,95}, A. Toia⁴⁷, N. Topilskaya⁵⁰, S. Tripathy³⁵, S. Trogolo¹⁶, V. Trubnikov², W.H. Trzaska⁹⁶, B.A. Trzeciak⁵¹, T.S. Tveter¹², A. Uras⁹¹, G.L. Usai¹⁴, G. Valentino⁹⁸, L.V.R. van Doremalen⁵¹, M. van Leeuwen⁵¹, P. Vande Vyvre²³, M. Vasileiou⁶³, V. Vechernin⁸², L. Vermunt⁵¹, O. Villalobos Baillie⁸¹, T. Virgili¹³, A. Vodopyanov⁵⁸, S.A. Voloshin¹⁰³, G. Volpe²², B. von Haller²³, I. Vorobyev⁷⁷, Y. Wang⁴, M. Weber⁸⁴, A. Wegrzynek²³, D.F. Weiser⁷⁸, S.C. Wenzel²³, J.P. Wessels¹⁰⁴, J. Wiechula⁴⁷, U. Wiedemann²³, J. Wilkinson³⁹, B. Windelband⁷⁸, M. Winn⁴⁶, N. Xu⁴, K. Yamakawa³¹, Z. Yin⁴, I.-K. Yoo¹¹, J.H. Yoon⁴⁵, A. Yuncu⁷⁸, V. Zaccolo^{15,43}, C. Zampolli²³, A. Zarochentsev⁸², B. Zhang⁴, X. Zhang⁴, C. Zhao¹², V. Zherebchevskii⁸², D. Zhou⁴, Y. Zhou⁴, Y. Zhou⁶⁸, G. Zinovjev².

¹ A.I. Alikhanyan National Science Laboratory (Yerevan Physics Institute) Foundation, Yerevan, Armenia

² Bogolyubov Institute for Theoretical Physics, National Academy of Sciences of Ukraine, Kiev, Ukraine

³ Bose Institute, Department of Physics and Centre for Astroparticle Physics and Space Science (CAPSS), Kolkata, India

⁴ Central China Normal University, Wuhan, China

- ⁵ Centro Fermi - Museo Storico della Fisica e Centro Studi e Ricerche ‘Enrico Fermi’, Rome, Italy
- ⁶ Chicago State University, Chicago, Illinois, United States
- ⁷ COMSATS University Islamabad, Islamabad, Pakistan
- ⁸ Creighton University, Omaha, Nebraska, United States
- ⁹ Department of Physics and Technology, University of Bergen, Bergen, Norway
- ¹⁰ Department of Physics, Aligarh Muslim University, Aligarh, India
- ¹¹ Department of Physics, Pusan National University, Pusan, Republic of Korea
- ¹² Department of Physics, University of Oslo, Oslo, Norway
- ¹³ Dipartimento di Fisica ‘E.R. Caianiello’ dell’Università and Gruppo Collegato INFN, Salerno, Italy
- ¹⁴ Dipartimento di Fisica dell’Università and Sezione INFN, Cagliari, Italy
- ¹⁵ Dipartimento di Fisica dell’Università and Sezione INFN, Trieste, Italy
- ¹⁶ Dipartimento di Fisica dell’Università and Sezione INFN, Turin, Italy
- ¹⁷ Dipartimento di Fisica e Astronomia dell’Università and Sezione INFN, Catania, Italy
- ¹⁸ Dipartimento di Fisica e Astronomia dell’Università and Sezione INFN, Florence, Italy
- ¹⁹ Dipartimento di Fisica e Astronomia dell’Università and Sezione INFN, Padova, Italy
- ²⁰ Dipartimento di Scienze e Innovazione Tecnologica dell’Università del Piemonte Orientale and INFN Sezione di Torino, Alessandria, Italy
- ²¹ Dipartimento DISAT del Politecnico and Sezione INFN, Turin, Italy
- ²² Dipartimento Interateneo di Fisica ‘M. Merlin’ and Sezione INFN, Bari, Italy
- ²³ European Organization for Nuclear Research (CERN), Geneva, Switzerland
- ²⁴ Faculty of Engineering and Science, Western Norway University of Applied Sciences, Bergen, Norway
- ²⁵ Faculty of Nuclear Sciences and Physical Engineering, Czech Technical University in Prague, Prague, Czech Republic
- ²⁶ Faculty of Science, P.J. Šafárik University, Košice, Slovakia
- ²⁷ Frankfurt Institute for Advanced Studies, Johann Wolfgang Goethe-Universität Frankfurt, Frankfurt, Germany
- ²⁸ Gauhati University, Department of Physics, Guwahati, India
- ²⁹ Helmholtz-Institut für Strahlen- und Kernphysik, Rheinische Friedrich-Wilhelms-Universität Bonn, Bonn, Germany
- ³⁰ High Energy Physics Group, Universidad Autónoma de Puebla, Puebla, Mexico
- ³¹ Hiroshima University, Hiroshima, Japan
- ³² Hochschule Worms, Zentrum für Technologietransfer und Telekommunikation (ZTT), Worms, Germany
- ³³ Horia Hulubei National Institute of Physics and Nuclear Engineering, Bucharest,

Romania

- ³⁴ Indian Institute of Technology Bombay (IIT), Mumbai, India
- ³⁵ Indian Institute of Technology Indore, Indore, India
- ³⁶ Indonesian Institute of Sciences, Jakarta, Indonesia
- ³⁷ INFN, Laboratori Nazionali di Frascati, Frascati, Italy
- ³⁸ INFN, Sezione di Bari, Bari, Italy
- ³⁹ INFN, Sezione di Bologna, Bologna, Italy
- ⁴⁰ INFN, Sezione di Cagliari, Cagliari, Italy
- ⁴¹ INFN, Sezione di Padova, Padova, Italy
- ⁴² INFN, Sezione di Roma, Rome, Italy
- ⁴³ INFN, Sezione di Torino, Turin, Italy
- ⁴⁴ INFN, Sezione di Trieste, Trieste, Italy
- ⁴⁵ Inha University, Incheon, Republic of Korea
- ⁴⁶ Institut de Physique Nucléaire d'Orsay (IPNO), Institut National de Physique Nucléaire et de Physique des Particules (IN2P3/CNRS), Université de Paris-Sud, Université Paris-Saclay, Orsay, France
- ⁴⁷ Institut für Kernphysik, Johann Wolfgang Goethe-Universität Frankfurt, Frankfurt, Germany
- ⁴⁸ Institut für Theoretische Physik, Johann Wolfgang Goethe-Universität Frankfurt, Frankfurt, Germany
- ⁴⁹ Institut für Theoretische Physik, Ruprecht-Karls-Universität Heidelberg, Heidelberg, Germany
- ⁵⁰ Institute for Nuclear Research, Academy of Sciences, Moscow, Russia
- ⁵¹ Institute for Subatomic Physics, Utrecht University/Nikhef, Utrecht, Netherlands
- ⁵² Institute of Experimental Physics, Slovak Academy of Sciences, Košice, Slovakia
- ⁵³ Institute of Physics, Homi Bhabha National Institute, Bhubaneswar, India
- ⁵⁴ Institute of Space Science (ISS), Bucharest, Romania
- ⁵⁵ Instituto de Ciencias Nucleares, Universidad Nacional Autónoma de México, Mexico City, Mexico
- ⁵⁶ Instituto de Física, Universidade Federal do Rio Grande do Sul (UFRGS), Porto Alegre, Brazil
- ⁵⁷ Johann-Wolfgang-Goethe Universität Frankfurt Institut für Informatik, Fachbereich Informatik und Mathematik, Frankfurt, Germany
- ⁵⁸ Joint Institute for Nuclear Research (JINR), Dubna, Russia
- ⁵⁹ KTO Karatay University, Konya, Turkey
- ⁶⁰ Laboratoire de Physique Subatomique et de Cosmologie, Université Grenoble-Alpes, CNRS-IN2P3, Grenoble, France
- ⁶¹ Lawrence Berkeley National Laboratory, Berkeley, California, United States
- ⁶² Nagasaki Institute of Applied Science, Nagasaki, Japan

- ⁶³ National and Kapodistrian University of Athens, School of Science, Department of Physics, Athens, Greece
- ⁶⁴ National Centre for Nuclear Research, Warsaw, Poland
- ⁶⁵ National Institute of Science Education and Research, Homi Bhabha National Institute, Jatni, India
- ⁶⁶ National Nuclear Research Center, Baku, Azerbaijan
- ⁶⁷ National Research Centre Kurchatov Institute, Moscow, Russia
- ⁶⁸ Niels Bohr Institute, University of Copenhagen, Copenhagen, Denmark
- ⁶⁹ NRC Kurchatov Institute IHEP, Protvino, Russia
- ⁷⁰ NRNU Moscow Engineering Physics Institute, Moscow, Russia
- ⁷¹ Nuclear Physics Group, STFC Daresbury Laboratory, Daresbury, United Kingdom
- ⁷² Nuclear Physics Institute of the Czech Academy of Sciences, Řež u Prahy, Czech Republic
- ⁷³ Petersburg Nuclear Physics Institute, Gatchina, Russia
- ⁷⁴ Physics Department, Panjab University, Chandigarh, India
- ⁷⁵ Physics Department, University of Jammu, Jammu, India
- ⁷⁶ Physics Department, University of Rajasthan, Jaipur, India
- ⁷⁷ Physik Department, Technische Universität München, Munich, Germany
- ⁷⁸ Physikalisches Institut, Ruprecht-Karls-Universität Heidelberg, Heidelberg, Germany
- ⁷⁹ Research Division and ExtreMe Matter Institute EMMI, GSI Helmholtzzentrum für Schwerionenforschung GmbH, Darmstadt, Germany
- ⁸⁰ Saha Institute of Nuclear Physics, Homi Bhabha National Institute, Kolkata, India
- ⁸¹ School of Physics and Astronomy, University of Birmingham, Birmingham, United Kingdom
- ⁸² St. Petersburg State University, St. Petersburg, Russia
- ⁸³ State University of New York, Stony Brook, New York, United States
- ⁸⁴ Stefan Meyer Institut für Subatomare Physik (SMI), Vienna, Austria
- ⁸⁵ SUBATECH, IMT Atlantique, Université de Nantes, CNRS-IN2P3, Nantes, France
- ⁸⁶ Suranaree University of Technology, Nakhon Ratchasima, Thailand
- ⁸⁷ Technische Universität München, Excellence Cluster 'Universe', Munich, Germany
- ⁸⁸ The Henryk Niewodniczanski Institute of Nuclear Physics, Polish Academy of Sciences, Cracow, Poland
- ⁸⁹ Universidade de São Paulo (USP), São Paulo, Brazil
- ⁹⁰ Universidade Estadual de Campinas (UNICAMP), Campinas, Brazil
- ⁹¹ Université de Lyon, Université Lyon 1, CNRS/IN2P3, IPN-Lyon, Villeurbanne, Lyon, France

- ⁹² Université de Strasbourg, CNRS, IPHC UMR 7178, F-67000 Strasbourg, France, Strasbourg, France
- ⁹³ Université Paris-Saclay Centre d'Études de Saclay (CEA), IRFU, Department de Physique Nucléaire (DPhN), Saclay, France
- ⁹⁴ University of Cape Town, Cape Town, South Africa
- ⁹⁵ University of Houston, Houston, Texas, United States
- ⁹⁶ University of Jyväskylä, Jyväskylä, Finland
- ⁹⁷ University of Liverpool, Liverpool, United Kingdom
- ⁹⁸ University of Malta, Msida, Malta
- ⁹⁹ University of Tennessee, Knoxville, Tennessee, United States
- ¹⁰⁰ University of Tokyo, Tokyo, Japan
- ¹⁰¹ University of Tsukuba, Tsukuba, Japan
- ¹⁰² Variable Energy Cyclotron Centre, Homi Bhabha National Institute, Kolkata, India
- ¹⁰³ Wayne State University, Detroit, Michigan, United States
- ¹⁰⁴ Westfälische Wilhelms-Universität Münster, Institut für Kernphysik, Münster, Germany
- ¹⁰⁵ Wigner Research Centre for Physics, Hungarian Academy of Sciences, Budapest, Hungary
- ¹⁰⁶ Yale University, New Haven, Connecticut, United States
- ¹⁰⁷ Yonsei University, Seoul, Republic of Korea

^I Also at: Dipartimento DET del Politecnico di Torino, Turin, Italy

^{II} Also at: Department of Applied Physics, Aligarh Muslim University, Aligarh, India

^{III} Also at: Institute of Theoretical Physics, University of Wrocław, Poland